Daily and cell type-specific membrane capacitance changes in mouse cortical neurons

Daniel Severin[1], Sofia Shirley[2], Alfredo Kirkwood[1,2] and Jorge Golowasch[3]

[1] Johns Hopkins Zanvyl Krieger Mind/Brain Institute, Rm 350 Dunning Hall, and
The Solomon H. Snyder Department of Neuroscience, Johns Hopkins University, 3400 N. Charles St., Baltimore, MD 21218
[2] Department of Biology, Johns Hopkins University, 3400 N. Charles St., Baltimore, MD 21218
[3] Department of Biological Sciences, New Jersey Institute of Technology, Newark, NJ 07102

Co-corresponding Authors:
Jorge Golowasch
Department of Biological Sciences, NJIT
100 Summit St, CKB 337
University Heights, NJ 07103
Phone: 973-596-8444, Fax: 973-596-5689
Email: Jorge.P.Golowasch@njit.edu

Alfredo Kirkwood
Johns Hopkins Zanvyl Krieger Mind/Brain Institute, Rm 350 Dunning Hall, and
The Solomon H. Snyder Department of Neuroscience
Johns Hopkins University, 3400 N. Charles St., Baltimore, MD 21218
Phone: 410-516-8640 / Fax: 410-516-8648
Email: kirkwood@jhu.edu

Running title: Daily regulation of membrane capacitance

Number of pages:
Number of figures:
Number of tables:

Keywords:

Circadian, Oscillators, Capacitance, Cortex, Hippocampus, Pyramidal cells, Granule cells, Electrophysiology

Abstract

Capacitance is a property of biological membranes determined by the properties of the lipid portion of the membrane, as well as morphological features of a cell. In neurons, membrane capacitance is a determining factor of synaptic integration, action potential propagation speed and firing frequency. Besides slow changes associated with increased morphological complexity during postnatal maturation, neuron membrane capacity is largely considered a stable, non-regulated constant magnitude. Here we report that in pyramidal cells of mouse primary visual cortex the membrane capacitance changes nearly two-fold between the start and the end of a daily light cycle. The changes are large, nearly two-fold in magnitude in pyramidal cells, but do not affect cortical parvalbumin-expressing inhibitory interneurons. We discuss possible functional and practical implications as well as potential mechanisms.

Introduction

The capacitance is a so-called passive property of the membrane and is a determinant factor of fundamental neuronal properties, such as action potential propagation speed (Hodgkin and Huxley 1952), synaptic integration (Baufreton et al. 2005; Martin 1976) and action potential firing frequency (Tewari et al. 2018). As summarized in equation 1,

$$C = \varepsilon \frac{A}{d} \quad [1]$$

capacitance depends not only on the dielectric constant (ε) of the insulating material (phospholipid bilayer in biological membranes), but also on the distance between the intracellular and the extracellular conductive milieu (d), and the membrane area (A). Membrane capacitance, C_m, changes during early postnatal development. In some neuronal types the capacitance becomes smaller as d increases due to myelin wrapping (Castelfranco and Hartline 2015) or perineuronal net (PNN) encapsulation (Tewari et al. 2018). On the other hand, in most neurons the capacitance increases as the membrane area increases during the maturation of structural complexity. It is common practice to report changes in capacitance as a proxy for changes in membrane surface (Haedo and Golowasch 2006; Perez-Garcia et al. 2021; Pineda et al. 2008; Royeck et al. 2008). In juveniles and adults, however, altered capacitance has only being reported for some mouse models of some neurological conditions or after traumatic insult (Adamsky et al. ; Akopian et al. 2016; Deng et al. 2021; Perez et al. 2021; Rangel-Barajas et al. 2021; Tewari et al. 2018). Indeed, after maturation is completed, membrane capacitance is largely considered to be a non-regulated, constant biophysical property of the neurons (however see (Scott et al. 2022)), since membrane

thickness (d) and the properties of membrane lipids, captured by the dielectric constant (ε), are also thought to be stable (Gentet et al. 2000).

Here we report a nearly two-fold daily oscillation of membrane capacitance in excitatory pyramidal cells of mouse visual cortex from layers 2/3. In contrast, parvalbumin-containing inhibitory interneurons (PV^+) of the same region show no such variations. We discuss the possible consequences for circuit stability, activity homeostasis and possible compensatory mechanisms that may operate simultaneously.

Methods

Animals

Both male and female, 20-26 days old PV-cre;Ai14 mice (Jackson Laboratories, Bar Harbor Maine) were used. All experiments were performed in accordance with the U.S. Public Health Service Policy on Humane Care and Use of Laboratory Animals, the National Institutes of Health Guidelines for the Care and Use of Animals in Research, and approved by the Institutional Animal Care and Use Committee at Johns Hopkins University, where the recordings were performed.

Animal light entrainment and slice preparation

Mice of both sexes were "entrained" for at least 2 weeks in light-controlled chambers with 12-hour light/dark cycles, scheduled to allow all experiments to be performed between 9 am and 8 pm. For slice preparation, the mice were removed from their cages ~10 minutes before the chosen circadian time (*Zeitgeber*, ZT) of study (ZT = 0/24, 6, 12 or 18 hours). The mice were first deeply anesthetized with isofluorane within 10 min after removal from their cages and then perfused transcardially with cold dissection buffer (5 ml at 10 ml/min) containing 212.7 mM sucrose, 5.0 mM KCl, 0.5 mM $CaCl_2$,10 mM $MgSO_4$ 1.25 mM NaH_2PO_4, 26 mM $NaHCO_3$, 10 mM glucose. After decapitation, brains were quickly removed, and acute sagittal brain slices (~300 µm) were made in ice-cold dissection buffer bubbled with a mixture of 5% CO_2 and 95% O_2. The slices were allowed to recover for 30 min at 30°C in dissection buffer and then for one hour at room temperature in artificial cerebrospinal fluid (ACSF): 124 mM NaCl, 5 mM KCl, 1.25 mM NaH_2PO_4, 26 mM $NaHCO_3$, 1.5 mM $MgCl_2$, 2.5 mM $CaCl_2$, 10 mM dextrose, and bubbled with a mixture of 5% CO_2 and 95% O_2.

All recordings were performed in a submerged recording chamber superfused with ACSF (30 ± 0.5°C, 2 ml/min). Synaptic blockers were included in the bath: 25 µM 6-cyano-7-nitroquinoxaline-2,3-dione (CNQX), 100 µM DL-2-amino-5 phosphonopentanoic acid, and 10 µM gabazine. Whole-cell voltage-clamp recordings were obtained from pyramidal cells identified by their shape and firing response to depolarizing current pulses (Fig. 1) in cortical layers 2 and 3, and from identified parvalbumin (PV) cells (fluorescent in these mice). We used borosilicate glass patch pipettes (3-6 MΩ) filled with intracellular solution containing the following: 130 mM K-gluconate, 10 mM KCl, 0.2 mM EGTA, 10 mM HEPES, 4 mM MgATP, 0.5 mM Na_3GTP, 10 mM Na-phosphocreatine (pH 7.2–7.3, 280–290 mOsm). Average input resistance of pyramidal cells was 81.9 ± 21.7 MΩ (range: 64.4 to 115.0 MΩ), and 103.0 ± 48.7 MΩ (range: 53.0 to 328.0 MΩ) of PV cells. Series resistance was < 20 MΩ (range 6-20MΩ), which was compensated at least 80% in every case. All drugs were purchased from either Sigma Aldridge (RRID:SCR_008988) or Tocris (RRID:SCR_003689).

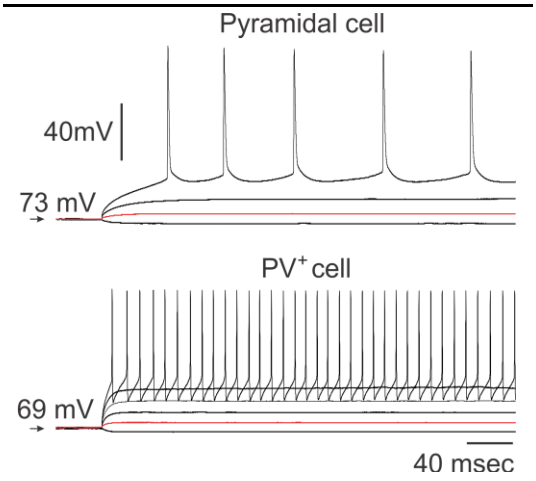

Figure 1. *Recordings of pyramidal and PV⁺ neuronal activity.* Pyramidal neurons (top) display a low frequency of action potential firing compared to PV⁺ cells (Bottom). Subthreshold voltage responses to current pulses (red traces) were fitted with a double exponential function from which membrane capacitance was derived as described in methods.

Capacitance measurements

Membrane capacitance was measured as described in Golowasch et al (2009). In that article we demonstrated mathematically and computationally that in anisotropic cells, such as highly branched neurons, only membrane capacitance estimates from current clamp (and not from voltage clamp) experiments are a good approximation to their actual total membrane capacitance. Using crab stomatogastric neurons, we also showed that in such cells voltage clamp estimates may underestimate membrane capacitance values by more than 10-fold in (Golowasch et al. 2009). Thus, here we used small depolarizing current pulses from a voltage slightly more depolarized than the average resting potential of the cells (Pyramidal cells: 70.2 ± 6.5 mV, N = 39; PV⁺ cells: 63.9 ± 5.2 mV, N = 45). The rationale for the chosen baseline voltage and the pulse amplitude was to avoid or minimize entering a voltage range where voltage-dependent currents are activated during the pulse (see (White and Hooper 2013)), thus remaining within levels where the cells respond passively. 2 second-long pulses were repeated 5 times and averaged to reduce noise. Pulses were then baseline subtracted and fitted with a double exponential function. The slowest exponential component corresponds to the cell's membrane charging curve (Rall 1977),

from which the time constant (τ_m), the membrane capacitance (C_m) and the membrane resistance (R_m) can be obtained (Golowasch et al. 2009; Rall 1977).

Statistical Analysis

Normally distributed data are reported as averages ± SD and were compared with *t*-Student tests or one-way ANOVA tests for independent samples. Non-normally distributed data are shown as medians, and 1st and 3rd quartiles, and were compared using Mann-Whitney *t*-tests, or Kruskal-Wallis tests. These statistical analyses and graphing were performed using SigmaStat and SigmaPlot, respectively (Systat Software, Inc., San Jose, CA. USA; RRID:SCR_010285).

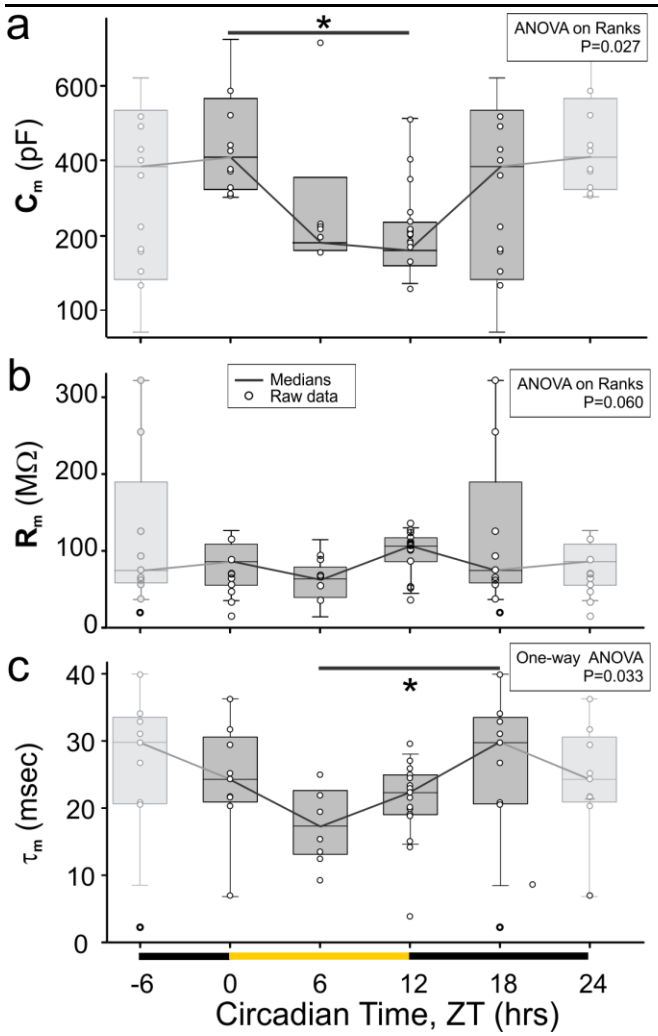

Figure 2. *Daily membrane parameter changes of cortical pyramidal neurons.* **a.** The membrane capacitance, C_m, of visual cortex layer 2/3 pyramidal cells is highest at ZT0 hours (beginning of the light phase) and lowest at ZT12 hours (beginning of the dark phase) (P = 0.027, Kruskal Wallis test on ranks). **b.** In the same cells R_m shows no statistically significant changes (P = 0.060, Kruskal Wallis test on ranks). **c.** Like C_m, the time constant (τ_m) of the pyramidal cells membrane also expresses statistically significant daily variations (P = 0.033, One way ANOVA). In these three panels individual cell values are represented by hollow circles. Data were obtained only at ZT0, ZT6, ZT 12 and ZT18 hours (dark symbols and boxes). The light gray symbols and boxes at ZT-6 and ZT24 hrs are repeated for enhanced visibility of the daily trend from the data measured at ZT18 and ZT0, respectively. Data are shown as superimposed boxes representing medians (horizontal line), 25th and 75th percentiles (boxes), and 10th and 90th percentiles (whiskers). The * indicates where the differences in the overall trends in **a** and **c** arise from (details in Table 1).

Results

Membrane capacitance of pyramidal cells varies as a function of time of day

Using the current clamp technique, we calculated the total membrane capacitance, C_m, of identified pyramidal cells from layer 2 and 3 of the visual cortex. Surprisingly, we observed a nearly two-fold C_m change between the beginning of the light period (ZT0) and the beginning of the dark period (ZT12) (Fig. 2a). These changes are statistically significant (P = 0.027, Kruskal-Wallis test on ranks), with the main difference arising between ZT0 and ZT12 (P < 0.05) (Table 1). We examined if the membrane resistance (R_m) also changes over a one day period but found no statistical significance to those changes (P = 0.060, Kruskal-Wallis test on ranks) (Fig. 2b). Considering that C_m and R_m both determine the time constant of the cell, we looked at changes in τ_m and also found statistically significant changes over the course of 24 hours (Fig. 2c) (P = 0.033, One-way ANOVA) (see Table 1 for details).

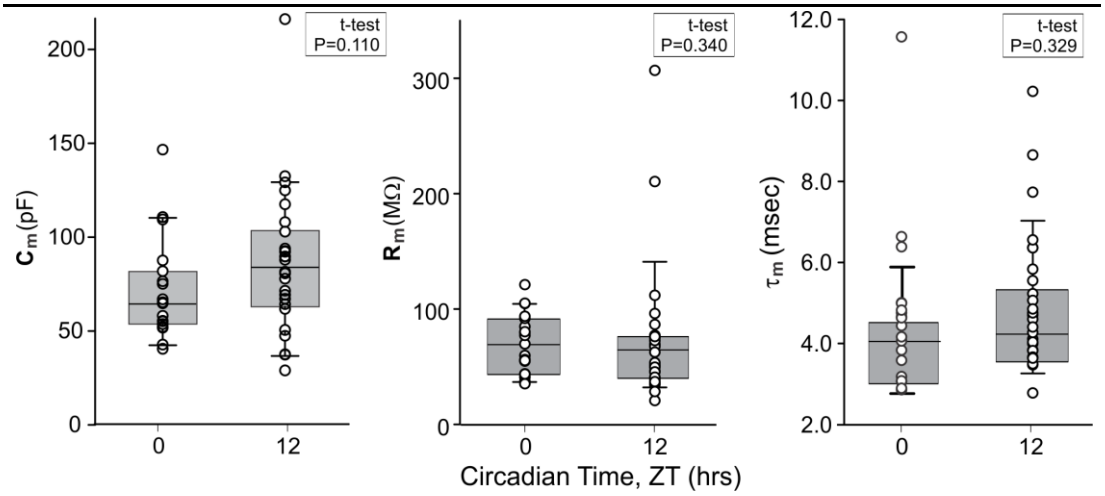

Figure 3. *Passive properties of PV⁺ neurons do not change with time of day*. PV⁺ inhibitory interneurons do not display any significant changes in *Cm* (P = 0.110, *t*-Student test, n=45, **left**), R_m (P = 0.340, *t*-Student test, n=45, **center**), or τ_m (P = 0.329, *t*-Student test, n=45, **right**) with time of day. Symbols have same meaning as in Fig.2.

Previous work has shown small but significant daily changes in PNN wrapping around parvalbumin-positive (PV^+) inhibitory cells that could result in capacitance changes (Pantazopoulos et al. 2020). Therefore, we asked if similar capacitance changes as those observed in pyramidal cells extend to other cell types, particularly, PV^+ inhibitory neurons. For this we focused on two key time points, ZT0 and ZT12. We observed no significant difference in C_m (P = 0.110, *t*-Student test, n = 45) (Fig. 3), R_m (P = 0.340, *t*-Student test, N = 38) or τ_m (P = 0.329, *t*-Student test, n = 45) when the same measurements were performed on PV^+ inhibitory neurons of the same cortical region.

Table 1. *Statistics of comparisons of pyramidal neuron parameters at different times during one day (ZT).* A Kruskal-Wallis analysis of variance on non-normally distributed samples was used. Medians, 1st and 3rd quartiles given. N = number of samples. For means and quartiles, first value is ZT0, second value is ZT12.

Parameter / Cell	Data structure	P	ZT	Means or Medians	SD or 1st/3rd quartiles	# cells (animals)
C_m (pF)	Non-Normal	**0.026**	0	375.6	318.3 / 480.1	9 (3)
			6	221.6	193.3 / 228.9	7 (2)
			12	209.8	182.5 / 260.0	16 (2)
			18	358.9	158.2 / 459.2	10 (2)
τ_m (msec)	Normal	**0.033**	0	24.1	8.3	
			6	16.7	5.6	
			12	21.9	4.2	
			18	27.1	9.3	
R_m (MΩ)	Non-Normal	0.051	0	65.7	41.5 / 81.1	
			6	56.1	56.1 / 90.3	
			12	88.2	88.2 / 119.3	
			18	60.4	60.4 / 192.0	

Table 2. *Statistics of comparisons of parvalbumin-positive (PV^+) inhibitory neuron parameters at ZT0 vs ZT12*. Mann-Whitney *t*-test on non-normally distributed samples (and medians, 1st and 3rd quartile given). N = number of samples. For means and quartiles, first value is ZT0, second value is ZT12.

Parameter / Cell	Data structure	P	Medians (N)	1st/3rd quartiles: ZT0, ZT12	# cells (animals)
C_m / PV^+ (pF)	Non-normal	0.110	83.9 (19) vs 64.4	103.3, 81.5 / 62.8, 53.3	19 (5)/26 (7)
τ_m / PV^+ (msec)	Non-normal	0.329	4.4 (19) vs 4.7	3.2, 3.8 / 5.0, 6.0	
R_m / PV^+ (MΩ)	Non-normal	0.340	64.9 (19) vs 69.6	40.3, 43.7 / 76.4, 91.8	
V_{rest} / PV^+ (mV)	Non-normal	0.136	-64.0 (19) vs -62.0	-66.0, -68.0 / -60.0, -62.0	

Discussion

Here we report a large daily oscillation of the membrane capacitance of visual cortex pyramidal cells. The changes occur with a maximum around ZT0 (beginning of the light period) and a minimum around ZT12 (end of the light period). These changes affect the time constant of the membrane, which also exhibits a large daily variation, with maximum and minimum closely tracking the membrane capacitance.

Functional implications

These changes can have profound consequences for the physiology of these neurons and the networks they are part of. There are three principal effects that changes in the time constant of a neuron can have: synaptic integration, action potential propagation speed and action potential spiking frequency. Synaptic integration is likely the most consequential of these effects. Synaptic integration plays a crucial role in the computation of inputs coming from different regions of the nervous system onto a target cell that allow them to integrate different sensory modalities (Spruston 2008) and different regions of the sensory space (Iacaruso et al. 2017). Our observations of a nearly two-fold change in capacitance (and membrane time constant) suggest that such integration should be quite different between the beginning and the end of the light (or dark) phase of the day. In particular, for a given region of the dendritic arbor, one can imagine that changes in capacitance can affect how proximal and distal inputs carry out spatial integration. For example, with a shorter time constant, two inputs arriving at different positions in a dendrite might summate only minimally, but summate more significantly if the capacitance, and thus the time constant of the membrane, increases.

It has been shown that the lifespan of gamma- (and perhaps other cortical) rhythms (Grillner et al. 2005; Hakim et al. 2018; Whittington et al. 2011) is highly dependent on the time constant of excitatory and inhibitory neurons in cortical microcircuits (Buzsaki and Wang 2012; Destexhe and Pare 1999; Traub et al. 1996). Thus, changes in membrane capacitance, and the membrane time constant, of any of the cells in such circuits, will affect the power, lifespan, as well as frequency of gamma rhythms, which will in turn affect the function and output of these circuits.

Localization of changes

Where in the dendritic tree does the capacitance change mainly emerge from? It clearly can't be the soma since the capacitance of the soma alone is about 10% of the total cell capacitance. With a two-fold change of total membrane, the soma simply can't account for it. Although pyramidal cells are very electrotonically compact (van Elburg and van Ooyen 2010), the axon is also unlikely to account for these changes since the method used is accurate only within approximately one electrotonic length of the cells (Golowasch et al. 2009), which axon likely exceed. Axons also have fewer branches that dendrites and thus less membrane. The electrotonic structure of these cells depends in part on the synaptic input it receives as well as the morphology and properties of the different regions of the cell (Bernander et al. 1991). This partially decouples different parts of the cell. Thus, the main sources of the capacitance changes measured likely depends on the levels of activity pyramidal cells receive at different times of the day. In any case, most of the capacitance changes we observe are likely to be dominated by changes at or near basal dendrites. The different computational roles that apical and basal dendrites perform, with apical thought to be primarily integration of sensory input, and basal primarily intra-cortical communication (Spruston 2008), is thus going to be affected differently by daily membrane capacitance changes.

Could daily changes in myelination of the axon account for this? The pyramidal cell axon, which is ensheathed by myelin (Peters and Sethares 1996; Tomassy et al. 2014) are unlikely to substantially contribute to the observed capacitance changes. Most of the cell's membrane is distributed in the (unmyelinated) dendritic tree, with axons being sparsely branched. Additionally, the accuracy of the C_m measurement method we used is only high within approximately one length constant (Golowasch et al. 2009), which excludes most of the axon.

Membrane capacitance changes are observed during the growth of a cell because capacitance is directly proportional to membrane surface [Eq. 1]. Membrane surface (and thus capacitance) changes also happen in the neocortex during synaptic remodeling following daily light/dark patterns; however, those changes are small (Jasinska et al. 2019). Membrane capacitance also varies due to wrapping of cells by tight apposition of other membrane layers such as those from Schwann cells and oligodendrocytes during myelination, or the formation of extracellular PNNs

around PV^+ interneurons (Carceller et al. 2022). Interestingly, we observe daily capacitance changes only in pyramidal neurons, which are not surrounded by PNNs in the cortex (Carceller et al. 2022; Tewari et al. 2018). PNNs are known to change their expression in a circadian manner (Pantazopoulos et al. 2020), and given their tight apposition on the membrane of certain neurons, influence membrane capacitance (Tewari et al. 2018). However, PNNs are observed only around PV^+ interneurons, which show no daily C_m changes, and not around pyramidal cells in cortex (Tewari et al. 2018; Wang and Fawcett 2012). Furthermore, the circadian changes of PNN structure observed in cortex has the opposite phase to what one would require to explain the observed C_m changes (Pantazopoulos et al. 2020).

Mechanisms

What cellular mechanisms could explain the large changes in membrane capacitance that we have observed? A two-fold change in membrane capacitance fits nicely with the possibility of pyramidal cells being wrapped by a single membrane layer of some adjacent cells in a manner analogous with myelination given the direct inverse proportionality of C_m with membrane thickness [Eq. 1]. However, as mentioned, myelination changes of the pyramidal cell axon are not likely to contribute significantly to this effect, and the rest of the cell is not myelinated. It is conceivable that shrinkage (towards the end of the light period) and expansion (towards the beginning of the light period) of the extracellular space (ECS) could produce an apparent two-fold membrane thickness variation that accounts for these results by producing close apposition of other cells on the pyramidal cell membrane. The effect of sleep-dependent variations of the ECS volume due to the glymphatic system (Ding et al. 2016; Jessen et al. 2015) daily dynamics could offer a conceivable explanation if the ECS nearly completely collapses at the end of the light period. However, it is not clear if the extend of the ECS volume shrinkage/expansion cycles mediated by the glymphatic system is sufficient to account for the full effect on membrane capacitance.

An additional contributing mechanism may be the growth and shrinkage of the cell surface itself. Again, a two-fold effect would need to be observed given the direct proportionality of capacitance and membrane area [Eq. 1]. This has never been observed. Only relatively minor circadian changes in synaptic number and shape, which would translate into similarly small changes in capacitance, have been

reported (de Vivo et al. 2017; Diering et al. 2017). However, it is conceivable that large amounts of membrane can be added or removed via bulk endocytosis or exocytosis (Cousin 2009) and that this could be regulated in a circadian or sleep-dependent fashion.

Yet another possible contributing mechanism may be circadian changes in dendrite diameter. A larger diameter would change the length constant of the dendrites by a factor equal to the square root of the diameter since

$$\lambda = \sqrt{\frac{d \cdot R_m}{2 \cdot R_i}}$$

(with R_m and R_i the membrane and axial resistivities and d the diameter). This would change the electrotonic structure of the cell and possibly allow the current clamp current injections used to estimate membrane capacitance to reach further along the dendrites and thus a larger extent of the membrane, and thus return a larger capacitance value.

It is unclear what mechanism can explain such large capacitance changes. However, it is very likely that no single mechanism is sufficient, and that a combination of these and other mechanisms are required to account for the observed changes. Further research will be required to answer this question.

Conclusion

Several important issues are opened by our rather surprising observations. One is what cellular mechanisms might explain the magnitude of the effects observed. Another is the functional consequences that such changes are inevitably going to have on both the individual neurons targeted (pyramidal cells), and the circuits they are part of. By extension, it is hard to avoid wondering what behavioral and cognitive effects these changes may exert. It is possible that compensatory changes due to circadian or sleep-induced ionic conductance regulation (Adamsky et al.), of ionic conductance co-regulation (Tran et al. 2019), or sleep or circadian synaptic changes (Bridi et al. 2020), are also involved. In either case, daily membrane capacitance changes introduce an important new variable in understanding the dynamics of neuronal and circuit activity in the nervous system.

References

Adamsky A, Kol A, Kreisel T, Doron A, Ozeri-Engelhard N, Melcer T, Refaeli R, Horn H, Regev L, Groysman M, London M, and Goshen I. Astrocytic Activation Generates De Novo Neuronal Potentiation and Memory Enhancement. *Cell* 174: 59-71 e14, 2018.

Akopian G, Barry J, Cepeda C, and Levine MS. Altered membrane properties and firing patterns of external globus pallidus neurons in the R6/2 mouse model of Huntington's disease. *J Neurosci Res* 94: 1400-1410, 2016.

Baufreton J, Atherton JF, Surmeier DJ, and Bevan MD. Enhancement of excitatory synaptic integration by GABAergic inhibition in the subthalamic nucleus. *J Neurosci* 25: 8505-8517, 2005.

Bernander O, Douglas RJ, Martin KA, and Koch C. Synaptic background activity influences spatiotemporal integration in single pyramidal cells. *Proc Natl Acad Sci U S A* 88: 11569-11573, 1991.

Bridi MCD, Zong FJ, Min X, Luo N, Tran T, Qiu J, Severin D, Zhang XT, Wang G, Zhu ZJ, He KW, and Kirkwood A. Daily Oscillation of the Excitation-Inhibition Balance in Visual Cortical Circuits. *Neuron* 105: 621-629 e624, 2020.

Buzsaki G, and Wang XJ. Mechanisms of gamma oscillations. *Annu Rev Neurosci* 35: 203-225, 2012.

Carceller H, Gramuntell Y, Klimczak P, and Nacher J. Perineuronal Nets: Subtle Structures with Large Implications. *Neuroscientist* 10738584221106346, 2022.

Castelfranco AM, and Hartline DK. The evolution of vertebrate and invertebrate myelin: a theoretical computational study. *J Comput Neurosci* 38: 521-538, 2015.

Cousin MA. Activity-dependent bulk synaptic vesicle endocytosis--a fast, high capacity membrane retrieval mechanism. *Mol Neurobiol* 39: 185-189, 2009.

de Vivo L, Bellesi M, Marshall W, Bushong EA, Ellisman MH, Tononi G, and Cirelli C. Ultrastructural evidence for synaptic scaling across the wake/sleep cycle. *Science* 355: 507-510, 2017.

Deng PY, Avraham O, Cavalli V, and Klyachko VA. Hyperexcitability of Sensory Neurons in Fragile X Mouse Model. *Front Mol Neurosci* 14: 796053, 2021.

Destexhe A, and Pare D. Impact of network activity on the integrative properties of neocortical pyramidal neurons in vivo. *J Neurophysiol* 81: 1531-1547, 1999.

Diering GH, Nirujogi RS, Roth RH, Worley PF, Pandey A, and Huganir RL. Homer1a drives homeostatic scaling-down of excitatory synapses during sleep. *Science* 355: 511-515, 2017.

Ding F, O'Donnell J, Xu Q, Kang N, Goldman N, and Nedergaard M. Changes in the composition of brain interstitial ions control the sleep-wake cycle. *Science* 352: 550-555, 2016.

Gentet LJ, Stuart GJ, and Clements JD. Direct measurement of specific membrane capacitance in neurons. *Biophys J* 79: 314-320, 2000.

Golowasch J, Thomas G, Taylor AL, Patel A, Pineda A, Khalil C, and Nadim F. Membrane capacitance measurements revisited: dependence of capacitance value on measurement method in nonisopotential neurons. *J Neurophysiol* 102: 2161-2175, 2009.

Grillner S, Markram H, De Schutter E, Silberberg G, and LeBeau FE. Microcircuits in action--from CPGs to neocortex. *Trends Neurosci* 28: 525-533, 2005.

Haedo RJ, and Golowasch J. Ionic mechanism underlying recovery of rhythmic activity in adult isolated neurons. *J Neurophysiol* 96: 1860-1876, 2006.

Hakim R, Shamardani K, and Adesnik H. A neural circuit for gamma-band coherence across the retinotopic map in mouse visual cortex. *Elife* 7: 2018.

Hodgkin AL, and Huxley AF. A quantitative description of membrane current and its application to conduction and excitation in nerve. *J Physiol* 117: 500-544, 1952.

Iacaruso MF, Gasler IT, and Hofer SB. Synaptic organization of visual space in primary visual cortex. *Nature* 547: 449-452, 2017.

Jasinska M, Jasek-Gajda E, Woznicka O, Lis GJ, Pyza E, and Litwin JA. Circadian clock regulates the shape and content of dendritic spines in mouse barrel cortex. *PLoS One* 14: e0225394, 2019.

Jessen NA, Munk AS, Lundgaard I, and Nedergaard M. The Glymphatic System: A Beginner's Guide. *Neurochem Res* 40: 2583-2599, 2015.

Martin AR. The effect of membrane capacitance on non-linear summation of synaptic potentials. *J Theor Biol* 59: 179-187, 1976.

Pantazopoulos H, Gisabella B, Rexrode L, Benefield D, Yildiz E, Seltzer P, Valeri J, Chelini G, Reich A, Ardelt M, and Berretta S. Circadian Rhythms of Perineuronal Net Composition. *eNeuro* 7: 2020.

Perez-Garcia P, Pardillo-Diaz R, Geribaldi-Doldan N, Gomez-Oliva R, Dominguez-Garcia S, Castro C, Nunez-Abades P, and Carrascal L. Refinement of Active and Passive Membrane Properties of Layer V Pyramidal Neurons in Rat Primary Motor Cortex During Postnatal Development. *Front Mol Neurosci* 14: 754393, 2021.

Perez H, Abdallah MF, Chavira JI, Norris AS, Egeland MT, Vo KL, Buechsenschuetz CL, Sanghez V, Kim JL, Pind M, Nakamura K, Hicks GG, Gatti RA, Madrenas J, Iacovino M, McKinnon PJ, and Mathews PJ. A novel, ataxic mouse model of ataxia telangiectasia caused by a clinically relevant nonsense mutation. *Elife* 10: 2021.

Peters A, and Sethares C. Myelinated axons and the pyramidal cell modules in monkey primary visual cortex. *J Comp Neurol* 365: 232-255, 1996.

Pineda RH, Knoeckel CS, Taylor AD, Estrada-Bernal A, and Ribera AB. Kv1 potassium channel complexes in vivo require Kvbeta2 subunits in dorsal spinal neurons. *J Neurophysiol* 100: 2125-2136, 2008.

Rall W. Core conductor theory and cable properties of neurons. In: *Handbook of Physiology (Section 1, The Nervous System I, Cellular Biology of Neurons)*, edited by Kandel ER. Bethesda, MD: American Physiological Society, 1977, p. 39-97.

Rangel-Barajas C, Boehm SL, 2nd, and Logrip ML. Altered excitatory transmission in striatal neurons after chronic ethanol consumption in selectively bred crossed high alcohol-preferring mice. *Neuropharmacology* 190: 108564, 2021.

Royeck M, Horstmann MT, Remy S, Reitze M, Yaari Y, and Beck H. Role of axonal NaV1.6 sodium channels in action potential initiation of CA1 pyramidal neurons. *J Neurophysiol* 100: 2361-2380, 2008.

Scott HL, Bolmatov D, Podar PT, Liu Z, Kinnun JJ, Doughty B, Lydic R, Sacci RL, Collier CP, and Katsaras J. Evidence for long-term potentiation in phospholipid membranes. *Proc Natl Acad Sci U S A* 119: e2212195119, 2022.

Spruston N. Pyramidal neurons: dendritic structure and synaptic integration. *Nat Rev Neurosci* 9: 206-221, 2008.

Tewari BP, Chaunsali L, Campbell SL, Patel DC, Goode AE, and Sontheimer H. Perineuronal nets decrease membrane capacitance of peritumoral fast spiking interneurons in a model of epilepsy. *Nat Commun* 9: 4724, 2018.

Tomassy GS, Berger DR, Chen HH, Kasthuri N, Hayworth KJ, Vercelli A, Seung HS, Lichtman JW, and Arlotta P. Distinct profiles of myelin distribution along single axons of pyramidal neurons in the neocortex. *Science* 344: 319-324, 2014.

Tran T, Unal CT, Severin D, Zaborszky L, Rotstein HG, Kirkwood A, and Golowasch J. Ionic current correlations are ubiquitous across phyla. *Sci Rep* 9: 1687, 2019.

Traub RD, Whittington MA, Colling SB, Buzsaki G, and Jefferys JG. Analysis of gamma rhythms in the rat hippocampus in vitro and in vivo. *J Physiol* 493 (Pt 2): 471-484, 1996.

van Elburg RA, and van Ooyen A. Impact of dendritic size and dendritic topology on burst firing in pyramidal cells. *PLoS Comput Biol* 6: e1000781, 2010.

Wang D, and Fawcett J. The perineuronal net and the control of CNS plasticity. *Cell Tissue Res* 349: 147-160, 2012.

White WE, and Hooper SL. Contamination of current-clamp measurement of neuron capacitance by voltage-dependent phenomena. *J Neurophysiol* 110: 257-268, 2013.

Whittington MA, Cunningham MO, LeBeau FE, Racca C, and Traub RD. Multiple origins of the cortical gamma rhythm. *Dev Neurobiol* 71: 92-106, 2011.